Journal of Geoscience and Environment Protection, 2026, 14(9), 26-45
https://www.scirp.org/journal/gep
ISSN Online: 2327-4344
ISSN Print: 2327-4336

Rock-Eval Kinetics Determination of Source Rocks from Muglad Basin, South Sudan

Thomas Michael Ali Mile[1,2]

[1]School of Applied and Industrial Sciences, University of Juba, Juba, South Sudan
[2]College of Natural Sciences, Makerere University, Kampala, Uganda
Email: amile7122@gmail.com

How to cite this paper: Mile, T. M. A. (2026). Rock-Eval Kinetics Determination of Source Rocks from Muglad Basin, South Sudan. *Journal of Geoscience and Environment Protection, 14,* 26-45.
https://doi.org/10.4236/gep.2026.149003

Received: August 8, 2026
Accepted: September 8, 2026
Published: September 11, 2026

Abstract

This study evaluates the organic richness, kerogen type, thermal maturity, and apparent activation energy distribution of source-rock cutting from wells in Muglad Basin. It applies Rock-Eval II pyrolysis results to compare Abu Gabra Formation and Baraka intervals. The study identifies the Abu Gabra Formation as the stronger oil-prone source interval and proposes that the Baraka Formation may also contribute to the petroleum system.

Keywords

Rock-Eval II Kinetics, Source Rocks, Muglad Basin, South Sudan

1. Introduction

The Muglad Basin covers an area of approximately 120,000 km^2, 600 km in length and 200 km in width. It is one of the largest intra-continental rift systems formed in world due to Central Africa Shear Zone (CASZ). The basin is oriented NW-SE, which expanded from the southern part of the Republic of Sudan to the northern part of the Republic of South Sudan.

During 1970s and 1980s, this area was widely explored by Exxon, Chevron, and Conoco among others. Only one giant oil field was found during 1975-2000, i.e., Unity Field in the Muglad Basin of South Sudan, discovered in 1980 (Figure 1), with the ultimate recoverable reserves of 900 million barrels. Many smaller fields were discovered in the Muglad Basin in South Sudan, such as El-naar, Toma south, El-toor and Munga field. Oil pay zones include the Lower Cretaceous strata and Upper Cretaceous in the Muglad Basin of South Sudan.

In November 1974, Chevron signed a concession agreement in the Democratic Republic of Sudan, covering an area of 516,000 km^2. Two large rift basins, Muglad and Melut, were both inside the block. Exploration operations began in 1975. Aeromagnetic and gravity data were collected and seismic data were recorded. The main drilling activities were concentrated in the Muglad Basin, where a series of oil fields had been discovered since 1979.

1.1. Regional Geology

1.1.1. Tectonic and Structural Setting

The Muglad Basin developed as a result of rifting and began to form in the late Jurassic to Cretaceous period. Breakup of the Pangea super-continent resulted in the formation of the Central African transcurrent slip zone. Movement on the transcurrent slip zone leads to the development of a regime of regional extension to one side of the slip zone, i.e., South Sudan, in the manner of perpendicular to the transcurrent slip zone, which is largely controlled by the orientation of faults within the basin. Most faults are normal faults with the trend in NW-SE direction and are perpendicular to the transcurrent slip zone. Basin growth is mainly the result of fault-controlled subsidence from late Jurassic to late Tertiary.

The basin evolution can be divided into a pre-rift phase, three rifting phases and a sag phase. First phase of rifting started in late Jurassic to early Cretaceous. Subsidence was accomplished by normal faulting parallel and sub-parallel to basin axes and margins. Second phase of rifting occurred during late Cretaceous and during the phase, when widespread deposition of lacustrine and flood plain clay stone and siltstone occurred. Final phase of rifting began in Paleocene.

In middle Miocene, basin areas entered an intracratonic sag phase of gentle subsidence accompanied by little faulting. Tectonically, the southern part of Heglig-Unity Ridge. The structures are dominated by the regional, deeply seated normal faults trending in the NW to SE direction (Figure 1).

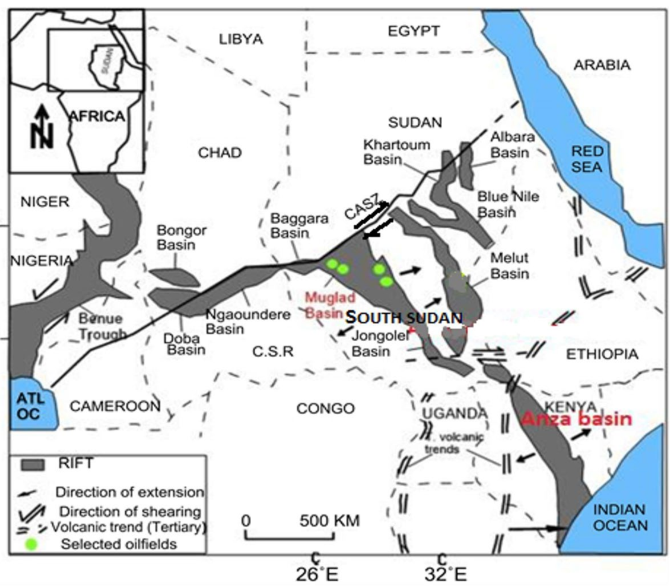

Figure 1. Map showing the location of the Muglad Basin of South Sudan as a part of the Central African Rift System.

1.1.2. Depositional Setting and Sedimentary Environment

Muglad Basin is characterized by more than 15,000 meters of non-marine clastic sediments. The combination of both continental (reservoir) and lacustrine (seal/source) rocks in conjunction with the tectonics has created favorable juxtaposition of source, reservoir and seal. Abu Gabra and Bentiu formations were deposited in Phase 1. Darfur Group and Amal formations deposited in Phase 2 and Nayil, Tendi, Adok and Zeraf formations were deposited in rift-phase 3.

The Abu Gabra formation was laid down as lacustrine shale in the early Cretaceous period and succeeded by a continental phase of meandering to braided channels of the Bentiu, completing Phase 1 of stratigraphy segence II.

This was succeeded by the lacustrine shales of the Aradeiba, continental deposits of the Zarqa and the mixed depositional environments of the Ghazal formation, with predominantly continental deposits of Baraka formation completing Phase 2 of stratigraphy segence II.

The formations, which comprise Phase 3 of stratigraphy segence II, Amal, Nayil, Tendi, Adok and Zeraf are of apredominantly continental phase, with the sands being deposited as braided and alluvial fans, the Nayil being the exception with mixed lacustrine and continental depositional environments as in Figure 2.

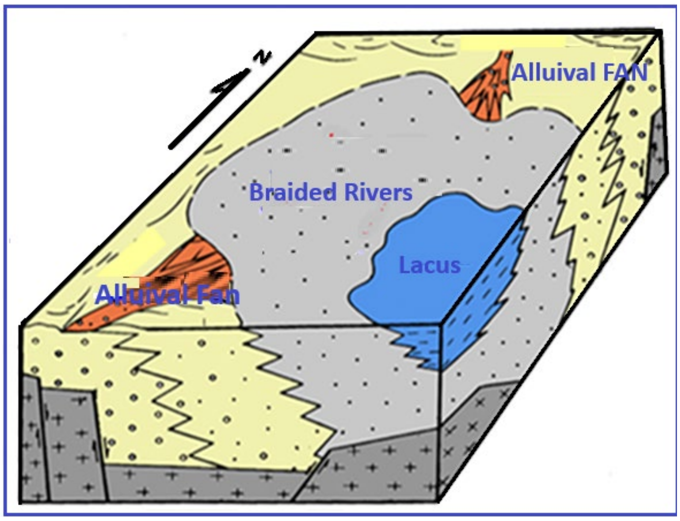

Figure 2. Generalized depositional model depicting non-marine environments operative during filling of Southern Sudan rift basins (Schull, 1988).

1.1.3. Stratigraphic History of the Rifting

The Muglad Basin has experienced three major extensional tectonic episodes. The early episode occurred approximately 140 to 95 Ma. in the Early Cretaceous. A second episode took place in Late Cretaceous, approximately between 95 - 65 Ma. While the last rifting episode occurred about 65 - 30 Ma in the Paleogene. The identification of three depositional cycles, which are regionally correlative, is the basis for the recognition of three separate rifting episodes. These depositional cycles, which are of explicit existence in the Muglad Basin, are indicated locally by delicate angular unconformity surfaces (McHargue et al., 1992).

Stratigraphically, each rift correlated depositional cycle starts about near the margins of the rift with basal sand overlaid by a shale-dominated interval, which reflects basin deepening. Each of these shaly intervals occurs as a base of coarsening upwards section grading from lacustrine shale into fluvial and lacustrine sandstone and mudstone when fully developed. Each of these shaly intervals occurs as a base of coarsening upwards section grading from lacustrine shale into fluvial and lacustrine sandstone and mudstone when fully developed. The later, in turn, is capped with the fluvial sandstones that are regionally extensive. The sediments of the three rifting episodes in the Muglad Basin attain a thickness of about 5400, 4200 and 5400 meters, respectively. After the Oligocene time, only sand-dominated sediments of about 750 meters were deposited in the basin.

The Muglad Basin stratigraphic succession represents a good example relating sedimentation to the contemporaneous tectonism. The stratigraphy can be seen as a result of rhythmic high sediment influx rate into depressions during episodes of cyclic alteration and subsidence patterns. The lithofacies association can be interpreted in light of different subsidence rates for various sub-basins. When subsidence was enormous during time of active rifting, shale-dominated sediments were deposited. While during time of low subsidence, most likely during thermal sag phases, sand-dominated sequence accumulated (**Figure 3**). Throughout each tectonic cycle, a broad area reflects an influence of the initial subsidence, although the subsidence rate was slow. This pattern may explain the existence of regional unconformity overlaid by the basal sand-dominated unit. This unit is sandiest at the margins of the rift and often shaly towards the depo-center.

The first depositional cycle (sand unit) has been penetrated only at the rift (Basin) margins, hence the geographic representation of this unit remains uncertain. On the contrary, the basal sand unit of the second depositional cycle (Upper Bentiu) and the third depositional cycle (Upper Amal) interfinger towards the axis of the rift with suspended-load fluvial and shaly lacustrine accumulations. This modality is thought to be applicable for the sand unit of the first depositional cycle. Following the accumulation of few hundred meters of the sand-dominated basal unit by the initial extension, the phase of active rifting initiated. This initiation is marked by a rapid subsidence of the hanging wall close to the main sub-basin boundary faults. During this rifting phase, the topographic relief is postulated to be at maximum while the sediment accumulation rate was high, yet unable to keep pace with the rapid fault-activated subsidence. At that time, the basin was characterized by close/sluggish drainage system linking a series of swaps and lakes. Each fault-bounded sub-basin behaved as a trap for the sediment where a thick shale-dominated section has been developed. Periods and areas of rapid subsidence were dominated by shales, either due to the sediments accumulation in long-lived outspread lakes or due to rapid descending of the deposited sediments beneath the erosional base and quick burial. In both cases, sediments suffered a little and/or winnowing after accumulation and the predominant shaly composition indicated the introduction of mostly fine clastics into the basin. Each of the three tectonic phases witnessed incoming coarse clastics from outside of the basin. This is supported by the presence of thick sandstone accumulations along the margins of the rift and their insignificance among the sediments accumulated near the intra-basinal highs during the main tectonic phases. The syn-rift sediments of the first tectonic cycle (Sharaf and Abo Gabra Formations) were associated with the extensive lacustrine shale (**Figure 3**) where the water of these lacustrine was stratified enough to prevent the accumulation and subsequent preservation of organic-reach kerogen shales representing the source rock of the oil in the Muglad Basin (Schull, 1988).

The second tectonic cycle syn-rift deposits (Lower Darfour Group) and the third tectonic syn-rift deposits (Nayil and Tendi Formations) again comprised mostly of lacustrine shales and fluvial over-bank deposits. These shales do not represent petroleum sources where they have been penetrated, while the sand deposited within these sequences represents premium reservoirs in the southern parts of the Muglad Basin. Towards the end of each tectonic cycle, the subsidence was altered gradually by a relatively slower rate of thermal down-warping basin-wide. The sediment influx during this stage took over the sub-basinal topography. Hence, the slow rate of subsidence allowed the continuous reworking by the bed-load streams, which penetrated the mud transported downstream outside the basin by the drainage system. The rest of the sediments were preserved as sheets of amalgamated fluvial sand throughout the whole basin (Lower Bentiu, Lower Amal, and Adok Formation). The distribution and thicknesses of sediments accumulated during each rifting phase of each tectonic cycle indicate that more influence of subsidence can be observed during first tectonic rifting cycle than in other cycles. Similar to the subsidence related to the tectonic rifting, the thermal rifting through the sag phase following the first tectonic cycle was greater than the other two subsequent cycles. Moreover, the thermal sag subsidence was positioned above the pro-ceeding subsidence of the below rifting phase for each tectonic cycle.

Although Muglad Basin is an important hydrocarbon province in South Sudan (**Figure 1**), but the origin of the oils and their source rock potential is still poorly known. There were reports on the presence of possible source rocks in the Muglad Basin that occur within the Early Cretaceous rock units (Mohamed et al., 2000; Zhang & Qin, 2011; Dou et al., 2013). The Early Cretaceous Abu Gabra Formation is the most important source rock present in the basin (Mohamed et al., 2000; Zhang & Qin, 2011; Dou et al., 2013). Abu Gabra organic-rich shales have been interpreted to be mainly oil-prone (Mohamed et al., 2000; Zhang & Qin, 2011; Dou et al., 2013; Makeen et al., 2015). Several studies have been undertaken on the basin concerning petroleum geology, stratigraphy, palynomorph assemblages,1D basin modelling, the tectonic history and structural geology of the basin, yet detailed bulk geochemical investigations on the produced crude oils and to correlate between oils and the potential source rocks in the Muglad Basin are lacking. The main objective of this study is to evaluate source rock potentiality for hydrocarbon generation of Early Cretaceous/Tertiary of the deeper parts of the Muglad rift basin and Quantify the thermal maturity.

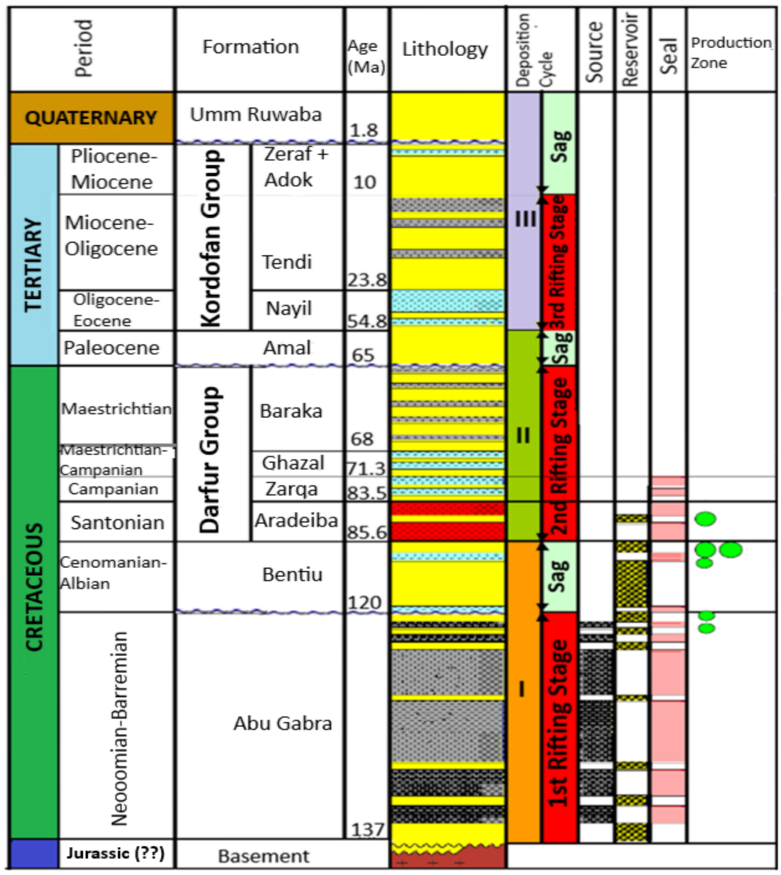

Figure 3. Generalized stratigraphic column of Fula Sub-Basin illustrating the formations, rifting cycles, and the petroleum system (Modified from Schull, 1988; Zhang & Qin, 2011; and Dou et al., 2013).

1.2. Rock-Eval II Pyrolysis Technique

The Rock-Eval pyrolysis instrument was developed by the Institut Français du Petrole. It provides a rapid semi-quantitative source rock analysis on small sample of rock by heating it, using special temperature program. It is an excellent screening technique for identifying possible source and reservoir intervals on which more detailed analysis should be performed. Rock-Eval programmed pyrolysis analysis was performed on whole-rock samples using the equipment Rock-Eval II analyzer. Five wells were selected for this method from Muglad Basin. The analytical results are discussed based on Table 1 and Table 2.

Evaluating Source Rock Using Rock-Eval II Parameters

Rocks are characterized according to the quantity of migrated or generated free hydrocarbons by cracking the OM in the rock. The quality of OM is defined in terms of kerogen types I through IV from HI/OI plots and the hydrocarbon type index (Hunt, 1979).

1) Quantity of Organic Matter

The quantity of organic matter is usually expressed in as Total Organic Carbon (TOC).

Table 1. Geochemical parameters describing source rock generative potential (quantity) after Peters and Moldowan (1993).

Quantity	TOC (wt %)	S_2 (mg HC/g rock)
Poor	<0.5	<2.5
Fair	0.5 - 1.0	2.5 - 5.0
Good	1.0 - 2.0	5.0 - 10.0
Very Good	>2.0	>10.0

2) Quality of Organic Matter (Kerogen Types)

The most important factor controlling the generation of oil and gas is the hydrogen content of the Organic Matter (OM) (Hunt, 1991).

Table 2. Geochemical parameters describing type of hydrocarbon generated (quality) after Peters and Moldowan (1993).

Type	Hydrogen index (mg HC/g TOC)	Rock-Eval (S_2/S_3)
Gas	50 - 200	1 - 5
Gas and Oil	200 - 300	5 - 10
Oil	>300	>10

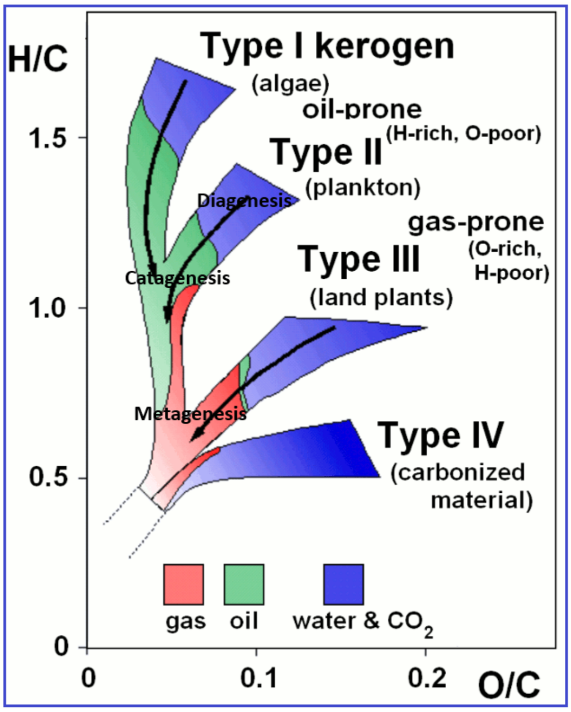

Figure 4. Modified Van Krevelen diagram showing the kerogen types.

Classifying organic matter type using the atomic H/C versus O/C ratio Van Krevelen diagram. This diagram was originally developed to characterize coals (Van Krevelen, 1961: Coal) during their thermal maturity or "coalification" (Tissot & Welte, 1984), and extended the use of Van Krevelen diagram from coals to include the kerogen dispersed in sedimentary rocks. The four principal types of kerogen include Type I (highly oil prone), Type II (oil prone), Type III (gas prone), and Type IV (inert) (**Figure 4**).

Type I kerogen has a high H/C ratio (≥1.5) and low O/C ratio (<0.1). It is rich in lipids, especially the long-chain aliphatics and has high petroleum potential derived from algal and bacterial remains. Type I kerogen is oil prone. Type II kerogen has intermediate H/C (1.5) and O/C (<0.2) ratios. It is derived primarily from planktonic and bacterial remains deposits. Its lipid content and oil potential are somewhat lower than type I kerogen. Type II is oil and gas prone. Type III kerogen has low H/C ratios (<0.1) and O/C (>0.3). It is rich in aromatic and poor in aliphatic structures. Its oil potential is poor, but it can be a source of gas (particularly methane). A fourth kerogen type (IV) has low H/C ratio and low to high O/C, which corresponds to the inertinite maceral group that generates little or no hydrocarbons during maturation.

3) Maturation of Organic Matter

Organic matter can be described as immature, mature, or postmatre, depending on its relation to the oil-generative window (Tissot & Welte, 1984). "Immature" organic matter has been affected only by diagenesis, including biological, physical, and chemical alteration. "Mature" organic matter has been affected by catagenesis, the thermal processes covering the temperature range between diagenesis and catagenesis. "Postmature" organic matter has been heated to such high temperature that it has been reduced to hydrogen-poor residue containing only small amounts of hydrocarbon gases.

4) T_{max} from Rock-Eval Data

Table 3 shows how to use the T_{max} from Rock-Eval pyrolysis to estimate thermal maturity. Rock-Eval T_{max} less than 435˚C indicates immature organic matter that has generated little or no petroleum. A T_{max} greater than 470˚C coincides with the wet-gas zone (Peters & Moldowan, 1993).

Table 3. Rock-Eval II geochmical and Ro parameters describing source rock thermal maturity (Peters & Moldowan, 1993).

Maturation Level	PI $[S_1/(S_1 + S_2)]$	T_{max} (˚C)	Ro (%)
Beginning of Oil Window	0.1	435 - 445	0.6
Peak Oil Window	0.25	445 - 450	0.9
End Oil Window	0.4	470	1.4

2. Materials and Methods

A total of about 25 cutting samples from five wells were selected for this study. The cutting samples from El Toor-6 about 16 samples from the depth of 2570 to 3020 in Abu Gabra interval, Unity-26 about 3 samples from the depth of 2865 - 2910 m in Abu Gabra interval, Amal-1 about 1 sample because of no enough core cutting at depth of 11,280 ft in Baraka interval. This well is located in Kaikang field and needs more resampling in future. In Azarag-1 about 4 samples at depth of 4850 - 4860 m to 5160 - 5170 m in Abu Gabra interval and also Khairat-1 has no enough sample only 1 sample at depth of 1900 m in Baraka formation, from Muglad Basin, South Sudan.

The Rock-Eval II instrument is capable of measuring hydrocarbons in a helium stream atmosphere and residual organic carbon by oxidation. The rock samples from five well cuttings (El Toor-6, Unity-26, Amal-1, Azarag-1 and Khairat-1) were molded into powered form. About 100 mg from each sample was first analyzed at 250˚C for 5 minutes that thermally distills organic compounds from C1 to about C32. The released hydrocarbons were measured by a flame ionization detector (FID) and the amount was recorded as S_1 (mg/g rock). Then, programmed pyrolysis from 250˚C to 600˚C at 25˚C/minute cracks the kerogen and heavy bitumen, yielding organic compounds, water and carbon dioxide as well as other gases. Then, the half flow of gas goes to the FID to measure the generated hydrocarbons as S_2 (mg HC/g rock) and half goes to a carbon dioxide trap. The gases flow into the carbon dioxide trap from 250˚C to 390˚C (from 390˚C to 600˚C, the evolved carbon dioxide is not collected). After completion of the programmed pyrolysis, the carbon dioxide trap is heated and the released gas is measured by a thermal conductivity detector (TCD), which was recorded as S_3 (mg HC/g rock). This amount of CO_2 is a function of the oxygen content of the organic matter. Then, the crucible was moved to another furnace where it was heated to about 590˚C in air (oxidizing atmosphere). The carbon dioxide and carbon monoxide evolved were measured as S_4 by the TCD (carbon monoxide is first converted to carbon dioxide using CuO catalysis). S_4 is the residual (inert) organic carbon and was added to S_1 and S_2 to calculate the total organic carbon content (TOC).

T_{max} (˚C) is the temperature where the maximum amount of S_2 hydrocarbons is generated. T_{max} is a function of kerogen type and thermal maturity. Rapid Rock-Eval II kinetic on a single, normal heating rate (25˚C/min) and fixed Arrhenius factor (1.48E14 sec^{-1}) was used to determine the kinetic energies. Then, the results are interpreted using petrographic software model 10.1029/2005GC000932.

3. Results and Discussion

3.1. Organic Richness

In general, the Abu Gabra and Baraka samples from Eltoor-6, Amal-1, Unity-26 recorded a good organic richness content ranging from 0.97 to 3.06% TOC (Table 4). Two other samples from Unity-26 (2875 and 2910 m) have much lower organic contents (0.21 and 0.37% TOC). The TOC values obtained from Abu Gabra samples in Azraq-1 and Baraka sample in Kairat-1 are poor to fair (TOC < 1%), as shown in Figure 5.

S_2 values from analyzed samples range from poor (<2 mg/g) to very good (>10 mg/g). The high S_2 values (**Figure 5**) are those samples from El-Toor-6, Amal-1 and Unity-26 (2865 m). Similar to TOC results, the low S_2 values were obtained from lower TOC samples from Azraq-1, Khairat-1 and Unity-26 (2875 and 2910 m).

3.2. Organic Matter Type and Thermal Maturity

The HI Vs T_{max} cross plot in **Figure 6** shows that all the samples are within mature zone. The cross plot also shows that there is large variation in HI values between samples, but very narrow distribution in terms of T_{max}. This could imply either, 1) all samples are made of mainly Type I kerogen that does not vary much with maturity, or 2) all samples have similar maturity in which case the HI difference reflects the changes in organic facies. In the latter case, this could mean that, there is a facies variation in Abu Gabra formation from a more oil-prone Type I in El-Toor-6 to a more oil gas-prone Type III in Azraq-1 and Unity-26.

Table 4. Rock-Eval II pyrolysis and organic carbon (TOC) content data.

Sample Depth	Formation	Lithology	TOC (wt %)	S_1 (mg/g)	S_2 (mg/g)	PI	HI	T_{max} (˚C)
				El-Toor-6				
2600 m	Abu Gabara	Shale	ND	0.16	20.56	0.01	ND	444
2630 m	Abu Gabara	Composite	2.17	0.16	12.96	0.01	597	444
2660 m	Abu Gabara	Shale	2.51	0.20	17.36	0.01	692	444
2690 m	Abu Gabara	Shale	1.88	0.17	11.40	0.01	506	443
2720 m	Abu Gabara	Composite	1.35	0.07	6.86	0.01	508	443
2750 m	Abu Gabara	Composite	ND	0.06	5.76	0.01	ND	444
2780 m	Abu Gabara	Composite	0.97	0.04	3.64	0.01	375	445
2810 m	Abu Gabara	Shale	1.01	0.06	4.70	0.02	465	445
2840 m	Abu Gabara	Shale	1.12	0.09	4.70	0.01	420	445
2870 m	Abu Gabara	Shale	ND	0.04	15.68	0.01	ND	444
2900 m	Abu Gabara	Shale	ND	0.06	7.45	0.01	ND	444
2930 m	Abu Gabara	Shale	ND	0.09	4.64	ND	ND	445
				Unity-26				
2865 m	Abu Gabara	Composite	1.53	0.08	4.92	0.02	322	447
2875 m	Abu Gabara	Shale	0.21	0.01	0.26	0.04	124	447
2910 m	Abu Gabara	Composite	0.31	0.02	0.14	0.13	38	445
				Amal-1				
11,280 ft	Baraka	Shale	3.06	0.11	9.74	0.01	316	440
11,340 ft	Baraka	Composite	2.63	0.19	7.74	0.03	281	438
				Azraq-1				
4850 ft	Abu Gabara	Composite	0.75	0.03	1.92	0.02	256	445
4910 ft	Abu Gabara	Shale/Silt	0.34	0.00	0.18	0.00	53	444

Continued

4940 ft	Abu Gabara	Composite	0.46	0.02	0.80	0.02	174	446
5170 ft	Abu Gabara	Shale	0.37	0.02	0.32	0.08	88	442
				Khairat-1				
1960 m	Baraka	Shale	0.69	0.02	0.78	0.03	113	439

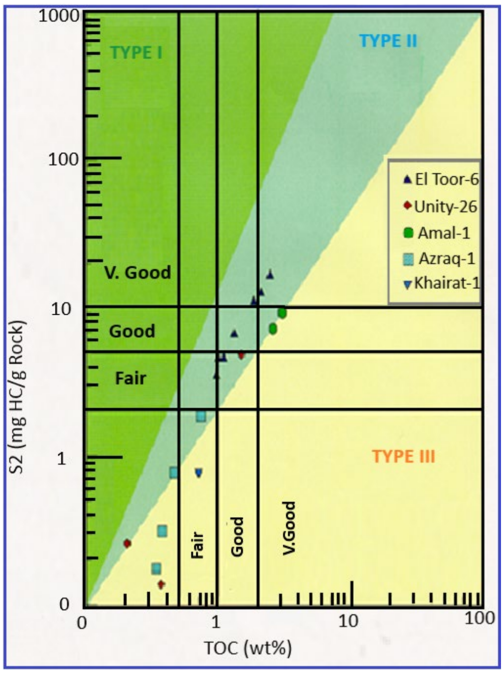

Figure 5. Plot of S_2 versus TOC for the study wells.

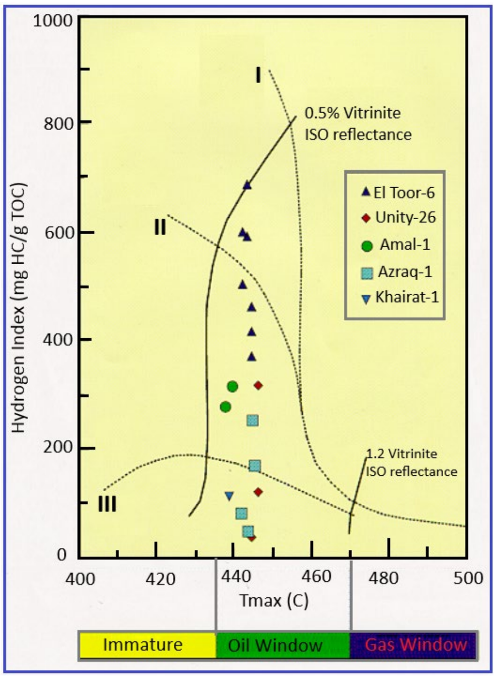

Figure 6. Plot of the study samples on a T_{max} versus hydrogen index diagram.

3.3. Kinetics Determination of the Origin of the Crude Oil

Tables 5-9 summarize kinetics data of all analyzed samples obtained using a single heating rate of 25˚C/min. The data are presented on histogram chart in Figures 7-10. All Abu-Gabra samples from El-toor-6 show a very narrow activation energies distribution, with dominating peaks at 55 Kcal/mol. This narrow variation of activation energies is typical lacustrine origin. This is in agreement with high HI values in these samples (Figure 6).

In Unity-26, the shallowest Abu-Gabra sample (2865 m) shows a very narrow distribution as well, indicating Type I kerogen. It has a dominating peak at 56 Kcal/mole. The same sample has high TOC, S_2 and HI values compared to the other two samples (2875 and 2910 m) from the same well. These samples (2875 and 2910 m) tend to have mixture of probably lacustrine Type I kerogen and Type III kerogen of continental origin, as indicated by a "tail" towards the higher activation energies.

In Azraq-1 sample, two samples (4850 - 4940 ft) are dominated by narrow distribution, while the other two samples (4910 - 4920 ft) and (5160 - 5170 ft) contain mixtures of narrow and broad distributions. With increasing in maturity, the presence of lower activation energy (<50 Kcal/mol) and increase in higher tail-end could also be contributed by the breakdown of kerogen.

Similar narrow and mixed distributions can be seen for the Baraka formation in Amal-1. There is a slight variation between the two Amail-1 samples, i.e., the maximum peak is at 56 and 55 kcal/mol for 11,280 and 11,340 ft, respectively. A sample from Khairat-1 shows a much broader distribution, possibly dominated by more gas-prone Type III kerogen.

Table 5. Kinetics data for El Toor-6 samples determined from normal Rock-Eval runs (25˚C/min) (Arrhenius factor, 1.48E14/sec^{-1}).

Depth (m) (Kcal/mole)	2600	2630	2660	2660	2690	2690	2720	2750	2780	2810	2815	28,400	2870	2900
45	0.4	0.6	0.5	0.5	0.6	0.6	0.1	0.1	0.3	0.5	1.1	0.3	0.2	0.4
46	0.2	0.3	0.3	0.3	0.4	0.4	0	0	0.2	0.5	0.5	0.1	0.1	0.3
47	0.1	0.1	0.1	0.1	0.3	0.3	0	0	0	0.7	0.6	0	0	0.4
48	0	0	0	0	0.1	0.1	0	0	0	0.3	1.1	0	0	0.5
49	0	0	0	0	0	0	0	0	0	0	1.1	0	0	0.1
50	0	0	0	0	0	0	0	0	0	0	0.1	0	0	0
51	0	0	0	0	0	0	0	0	0	0	0	0	0	0
52	0	0	0	0	0	0	0	0	0	0	0	0	0	0
53	0	0	0	0	0	0	0	0	0	0	0	0	0	0
54	0	0	0	0	0	0	0	0	0	0	0	0	0	0
55	12	5	8.5	2.8	13.7	7.2	13.2	2.1	0	0	12.1	4.3	3.2	3.8

Continued

56	86.6	93.7	90.5	96.1	84.6	91	86.7	97.7	96.1	97.6	82.8	94.9	96.4	93.8
57	0	0	0	0.1	0	0	0	0	1.6	0	0	0.1	0	0.1
58	0	0	0	0	0	0	0	0	0	0	0	0	0	0
59	0	0	0	0	0	0	0	0	0.1	0	0	0	0	0
60	0	0	0	0	0	0	0	0	0.6	0	0	0	0	0
61	0	0	0	0	0	0	0	0	0.7	0	0.1	0	0	0.1
62	0.1	0	0	0	0	0	0	0	0.2	0.1	0.1	0	0	0.2
63	0.1	0	0	0	0	0.1	0	0	0.1	0.1	0.1	0	0	0.1
64	0.1	0	0	0	0	0.1	0	0	0	0.1	0.1	0	0	0.1
65	0.1	0	0	0	0	0.1	0	0	0	0	0.1	0	0	0
66	0.1	0	0	0	0	0	0	0	0	0	0.1	0	0	0
67	0	0	0	0	0	0	0	0	0	0	0	0	0	0
68	0	0	0	0	0	0	0	0	0	0	0	0	0	0
69	0	0	0	0	0	0	0	0	0	0	0	0	0	0

Table 6. Kinetics data for Unity-26 samples determined from normal Rock-Eval II runs (25˚C/min) (Arrhenius factor, 1.48E14/sec^{-1}).

Depth (m) (Kcal/mole)	2865	2875	2910
45	0	2.8	16.4
46	0	0.4	1.3
47	0	0.5	4.1
48	0	0.6	11
49	0	0.4	5.6
50	0	0	2
51	0	0	0.3
52	0	0	0
53	0	0	0
54	0	0	0
55	0	0.1	6
56	74.9	63.9	35.9
57	23	17.8	9.7
58	0.1	2.6	2.8
59	0	2.5	2
60	0.1	3.6	1.9
61	0.4	2	0.8
62	0.6	0.8	0.2
63	0.4	0.5	0

Continued

64	0.2	0.4	0
65	0.1	0.4	0
66	0.1	0.2	0
67	0	0.1	0
68	0	0.1	0
69	0	0	0

Table 7. Kinetics data for Azraq-1 samples determined from normal Rock-Eval II runs (25˚C/min) (Arrhenius factor, 1.48E14/sec^{-1}).

Depth (m) (Kcal/mole)	4850 - 4860	4910 - 4920	4930 - 4940	5160 - 5170
45	1	4.4	2.1	3.7
46	0.4	0.2	0.4	1
47	0.5	0.5	0.5	1.5
48	1.1	1.8	0.8	1.9
49	0.5	1.3	1.3	2.5
50	0	1.6	0.4	2.8
51	0	1.7	0	0.6
52	0	0.5	0	0
53	0	0.1	0	0
54	0	0.2	0	0.2
55	1.2	10.8	0	21.5
56	90.8	59.2	82.3	43.7
57	0.5	9.3	8	7.8
58	0.1	2.9	0.7	4
59	0.7	2.9	1.1	4.1
60	1.6	1.6	1.5	2.5
61	0.9	0.4	0.7	1.2
62	0.3	0.1	0.2	0.5
63	0.1	0.1	0	0.2
64	0.1	0.1	0	0.1
65	0	0.1	0	0.1
66	0	0.1	0	0
67	0	0	0	0
68	0	0	0	0
69	0	0	0	0

Table 8. Kinetics data for Amal-1 samples determined from normal Rock-Eval II runs (25˚C/min) (Arrhenius factor, 1.48E14/sec^{-1}).

Depth (ft)	11,280	11,280 (Repeat)	11,340	11,340 (Repeat)
45	0.3	0.4	0.9	1.1
46	0.1	0.2	0.3	0.3
47	0	0.2	0.3	0.2
48	0	0.2	0.5	0.4
49	0	0	0.8	0.8
50	0	0	0.6	0.9
51	0	0	0.1	0.1
52	0	0	0	0
53	0	0	0	0
54	0	0	0.4	1.3
55	27.5	29.6	50	51.2
56	59.3	55.1	28.9	25
57	1.6	2.2	4.8	6
58	1.1	1.5	3.1	3.9
59	3	3.2	2.9	2.9
60	2.7	2.7	1.9	1.7
61	1.1	1.2	1	0.9
62	0.5	0.6	0.7	0.6
63	0.4	0.5	0.6	0.6
64	0.6	0.6	0.7	0.6
65	0.7	0.8	0.7	0.7
66	0.5	0.6	0.5	0.5
67	0.2	0.3	0.2	0.2
68	0.1	0.1	0.1	0.1
69	0	0	0	0

Table 9. Kinetics data for Khairat-1 samples determined from normal Rock-Eval II runs (25˚C/min) (Arrhenius factor, 1.48E14/sec^{-1}).

Depth (m) (Kcal/mole)	1960
45	1.6
46	0.8
47	1
48	0.9
49	0.9
50	1.4
51	2.1

Continued

52	2.1
53	2.5
54	6.5
55	23.7
56	28
57	10.3
58	3.9
59	3.4
60	4.1
61	2.8
62	1.4
63	0.9
64	0.7
65	0.5
66	0.2
67	0.1
68	0
69	0

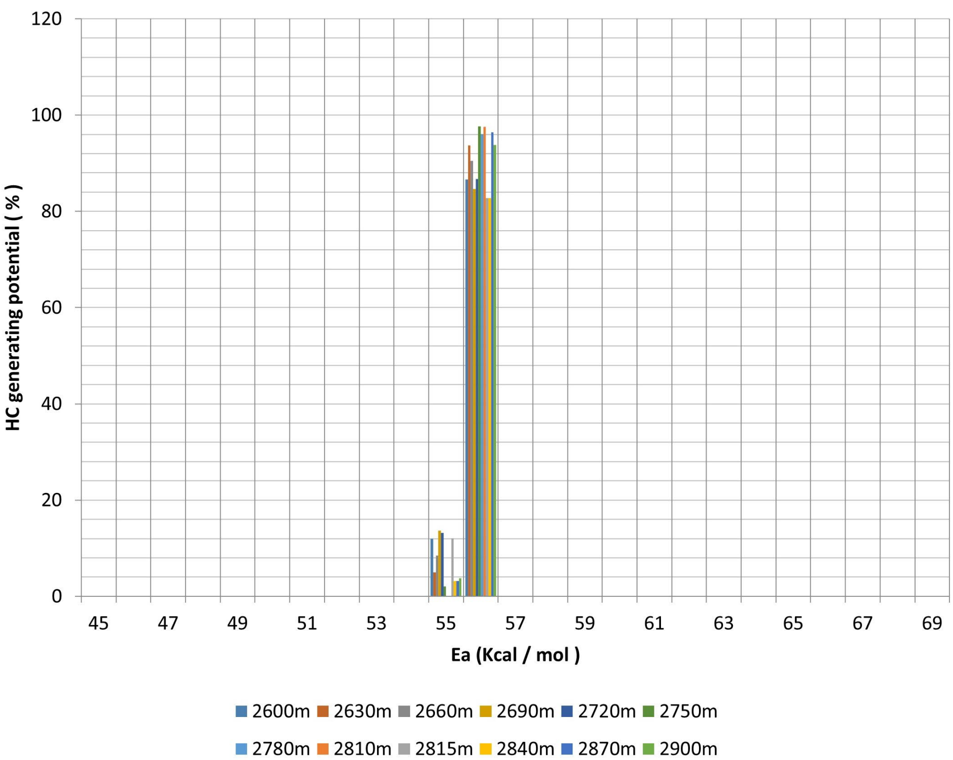

Figure 7. Distribution activation energies for El-Toor-6, determined from normal Rock-Eval II runs (25˚C/min) at different depths.

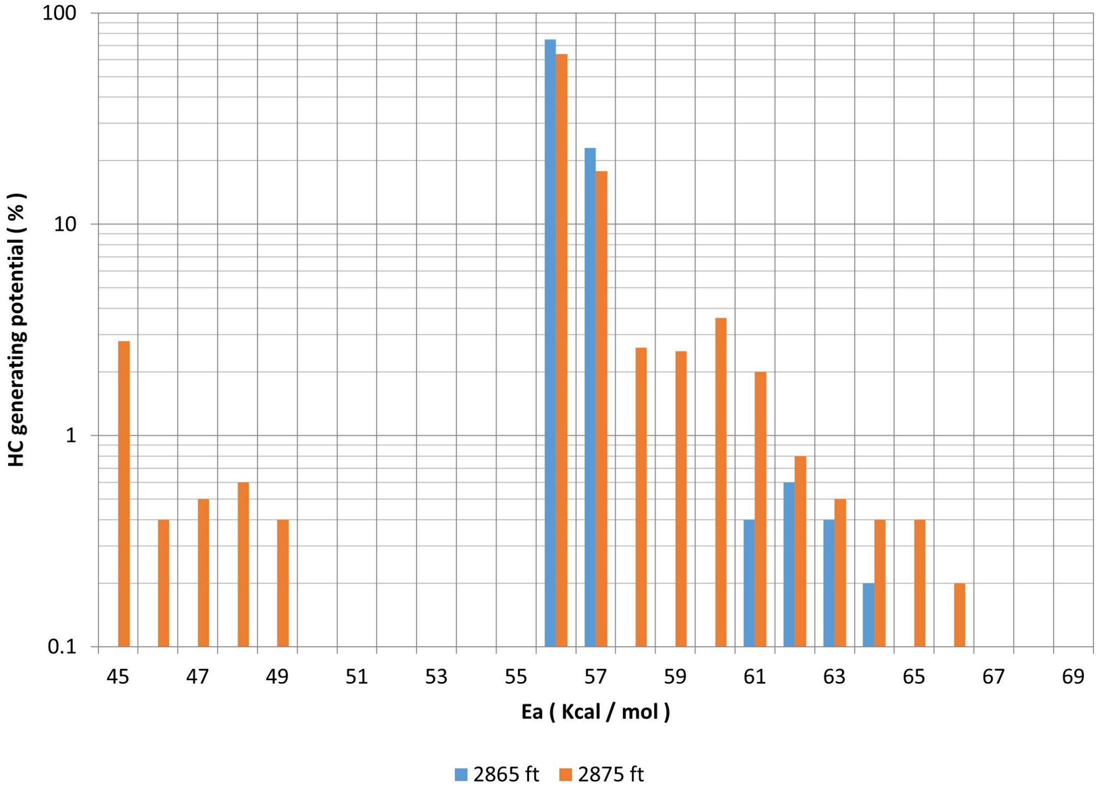

Figure 8. Distribution activation energies for Amail-1, determined from normal Rock-Eval II runs (25˚C/min) at different depths.

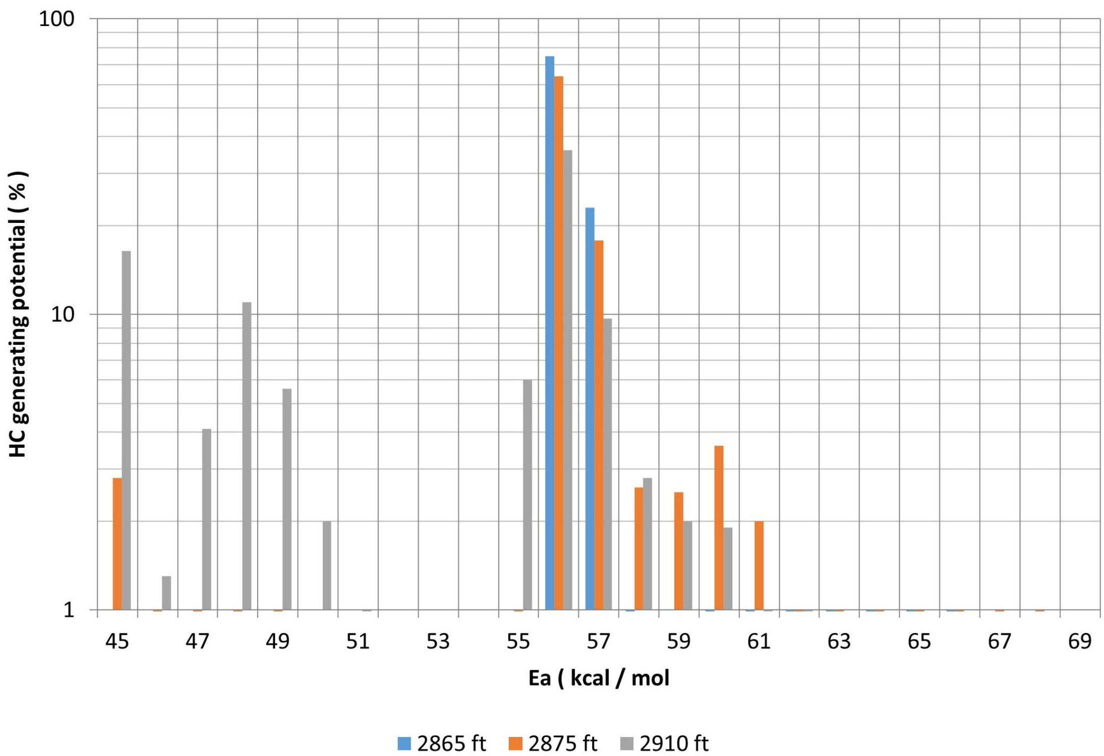

Figure 9. Distribution activation energies for Unity-26, determined from normal Rock-Eval II runs (25˚C/min) at different depths.

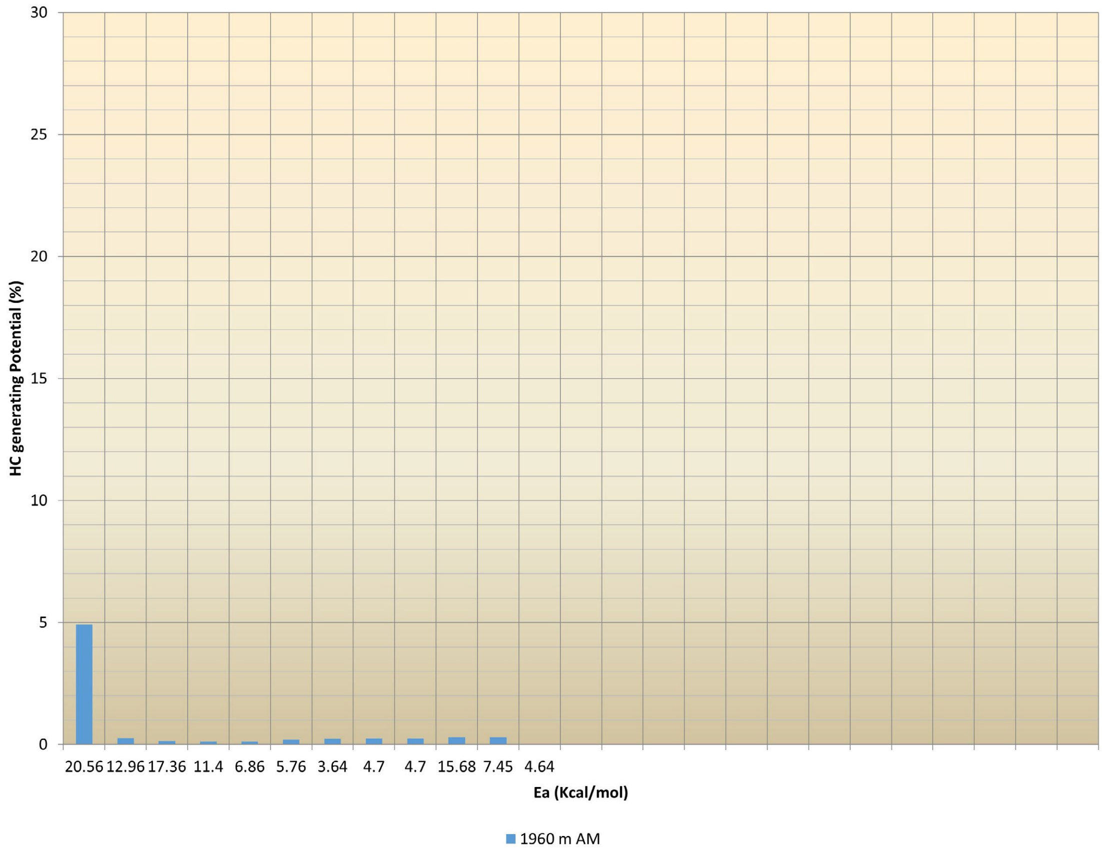

Figure 10. Distribution activation energies for Kariat-1, determined from normal Rock-Eval II runs (25˚C/min) at different depths.

4. Conclusion

The main conclusions derived from this study are as follows:

The Abu Gabra samples in El Toor-6 and Unity-26 at 2865 m have a very narrow activation energies distribution suggesting type I lacustrine origin. S_2, HI and TOC support the good source potential of this formation.

In other Abu Gabra samples from Azraq-1 and Unity-26 at 2875 and 2910 m, broader distribution is present, suggesting a possible mixture of more gas-prone kerogen. The S_2, HI and TOC values for these samples are much lower than the samples having narrower distribution.

The Baraka samples from Amal-1 show some possible mixed assemblages, between dominant Type I kerogen with some gas-prone type III kerogen, having broader activation energy distribution and lower source potential.

This study may have concluded that there are two possible source rocks within Muglad Basin. Baraka formation probability is one of the source rocks.

5. Recommendations for Additional Work

Based on observations made during this study, it is apparent that further work should be conducted in a number of areas in order to better delineate areas for future exploration. Suggestions accompanied by a brief explanation of the rationale behind each endeavor follows:

1) The oil from Baraka samples of Amal-1 should be resampled if at all possible. Although it is quite possible that the Amal-1 oil has the same source as all of the other oils from the Muglad Basin, it is important to note that several differences are present, as is explained fully in this study. Unfortunately, the sample quality was quite poor, resulting in answers that are less than definitive. If indeed, there is another source in the Kaikang area, it is extremely important to determine that as early as possible, if cost allows.

2) The geochem-sampling program should be revisited. It is apparent that in the past, much of the data sampled and then measured has been of little value to any sort of analysis. Sampling in block 4 should be consistent and thorough with a goal of arriving at a reliable maturation profile. Additional rock-eval measurements from units younger than Aradeiba are probably unwarranted in as much as the wells drilled will not sample these units in the right facies and, as demonstrated in this study, only Baraka and older units have any hope of having reached maturity (assuming typical lacustrine source).

3) Laboratory procedures need to be addressed. The reporting procedure from study is less than adequate and not in keeping with that provided by world-class laboratories. As such, it is impossible to discern the validity of any given measurement.

Conflicts of Interest

The author declares no conflicts of interest regarding the publication of this paper.

References

Dou, L. R., Cheng, D. S., Li, Z., Zhang, Z. W., & Wang, J. C. (2013). Petroleum Geology of the Fula-Sub Basin, Muglad Basin, Sudan. *Journal of Petroleum Geology, 36,* 43-59. https://doi.org/10.1111/jpg.12541

Hunt, J. M. (1979). *Petroleum Geochemistry and Geology* (1st ed.). Freeman.

Hunt, J. M. (1991). Generation of Gas and Oil from Coal and Other Terrestrial Organic Matter. *Organic Geochemistry, 17,* 673-680. https://doi.org/10.1016/0146-6380(91)90011-8

Makeen, Y. M., Abdullah, W. H., Hakimi, M. H., & Mustapha, K. A. (2015). Source Rock Characteristics of the Lower Cretaceous Abu Gabra Formation in the Muglad Basin, Sudan, and Its Relevance to Oil Generation Studies. *Marine and Petroleum Geology, 59,* 505-516. https://doi.org/10.1016/j.marpetgeo.2014.09.018

McHargue, T. R., Heidrick, T. L., & Livingston, J. E. (1992). Tectonostratigraphic Development of the Interior Sudan Rifts, Central Africa. *Tectonophysics, 213,* 187-202. https://doi.org/10.1016/0040-1951(92)90258-8

Mohamed, A. Y., Iliffe, J. E., Ashcroft, W. A., & Whiteman, A. J. (2000). Burial and Maturation History of the Heglig Field Area, Muglad Basin, Sudan. *Journal of Petroleum Geology, 23,* 107-128. https://doi.org/10.1111/j.1747-5457.2000.tb00486.x

Peters, K. E., & Moldowan, J. M. (1993). *The Biomarker Guide*. New Jersey.

Schull, T. J. (1988). Rift Basins of Interior Sudan: Petroleum Exploration and Discovery. *AAPG Bulletin, 72,* 1128-1142. https://doi.org/10.1306/703c9965-1707-11d7-8645000102c1865d

Tissot, B. P., & Welte, D. H. (1984). Petroleum Formation and Occurrence (2nd ed., 699 p). Springer.

Van Krevelen, D. W. (1961). *Coal: Typology-Chemistry-Physics-Constitution* (170 p). Elsevier Science.

Zhang, Y., & Gu, Q. (2011). Petroleum System of the Fula Depression at the Muglad Basin in the Central African Fault Zone. *Journal of Earth Science, 22,* 363-370. https://doi.org/10.1007/s12583-011-0188-3